Injection Strategy and EGR Optimization on a Viscosity-Improved Vegetable Oil Blend Suitable for Modern Compression Ignition Engines

2020-01-2141

Injection Strategy and EGR Optimization on a Viscosity-Improved Vegetable Oil Blend Suitable for Modern Compression Ignition Engines

Abstract

To comply with the ambitious CO_2 targets of the European Union, greenhouse gas emissions from the transport sector should be eliminated by 2050. Incremental powertrain improvement and electrification are only a part of the solution and need to be supplemented by carbon-neutral fuels. Due to the high technology readiness level, biofuels offer a short-term decarbonization measure. The high process energy demand for transesterification or hydrotreating however, hinders the well-to-wheel CO_2 reduction potential of current market biodiesels. An often-raised, economically and energetically feasible alternative is to use unprocessed oils with viscosity and cold-properties improvers instead. The present work investigates the suitability of one such biofuel (Plantanol^{TM}) for advanced common rail engines operating in a partially premixed compression ignition mode. Preliminary investigations are carried out on a Euro VIb light-duty car engine. The main focus is on the influence of the fuel blend on the soot/NO_X emission trade-off without changing the engine control maps. Single-cylinder engine tests are then focused on the optimization potential of injection parameters and external EGR to reach optimum performance-emissions trade-off on the new fuel. The results highlight that at the factory map setting, without EGR, biofuel offers slightly reduced thermal efficiency with respect to diesel, as a joint effect of retarded combustion and elevated THC and CO emissions. NO_X emissions are reduced by 20% at both non-EGR and to 25% EGR operation. With injection parameters optimization, the combustion phasing can be adjusted to diesel-like values while keeping the NO_X reduction benefits. The tested bio-oil blend is however sensitive to EGR, where increasing the recirculation rate retards the combustion while the soot emissions increase almost five-fold over the non-EGR baseline.

Introduction

The last ten years witnessed a stunning increase in the global production of renewable fuels. Assuming that the current growth rate (on average 7.8% per annum) is sustained, the share of renewable fuels in primary power generation will have increased to around 15% by 2040 [1]. While the growth of renewables can cover only half of the global increase in fuel demand, it is far from the ambitious CO_2 reduction targets of the 2015 Paris Agreement.

Due to high energy density and power requirements in the heavy-duty road and marine transport in particular, diesel engines are bound to remain the prime mover in the coming 30 years. The current market price of biodiesels – fatty acid methyl esters (FAMEs) and hydro-treated vegetable oils (HVOs), makes them barely competitive with fossil diesel fuel (DF) [2]. Furthermore, their well-to-wheel CO_2 reduction potential is hindered by energy-demanding refining processes. Recent studies [3-6] re-emphasize the advantages of using straight vegetable oils (SVOs) instead of biodiesel. Hossain and Davies [3] argue that the produced-to-consumed energy ratio for SVO is much higher than for refined biodiesels. Agrawal et al. [4] compared the production costs of linseed oil with esters obtained from the same feedstock. FAME proved to be 10% more costly on an energy basis when compared to SVO. Ortner et al. [5] used life cycle assessment modeling to compare the greenhouse gas emissions of different bio-oil feedstock and biodiesel produced from them. The general observation was that the processed vegetable oils generate the highest amounts of CO_2 over the whole lifecycle. Esteban et al. [6] arrived at similar conclusions. They also found that SVOs generate significantly lower well-to-wheel emissions of toxic compounds than their esters, despite FAMEs tank-to-wheel emissions being more favorable.

The elevated brake specific total hydrocarbons (THC) and CO emissions combined with increased fuel consumption were reported in the bulk of compression ignition (CI) engine applications of SVOs [7]. This primarily results from the fact that the physicochemical parameters of SVO do not match the diesel-optimized design parameters of injection and combustion systems. This is predominantly related to high viscosity, usually above 30 mm^2/s (at 40 °C), causing worse fuel atomization and reduced oxygen entrainment into the developing spray. High viscosity together with reduced cetane number result in extended ignition delay (physical and chemical, respectively) when SVO is combusted [8]. Both atomization and retarded combustion contribute – in the long run – to engine operational issues related to injector coking and lube oil dilution [9]. Engine-out NO_X emissions are typically reported to be 10%-30% lower for neat SVO compared to the diesel baseline on legacy engines [10].

The afore-mentioned adverse effects of SVO on combustion can be mitigated either by fuel blending, addification, or partially, by combustion system optimization (both hardware and control). The first strategy has been thoroughly investigated, so for a comprehensive review of blending strategies, the reader is referred to the work by Misra and Murthy [7]. The addification mainly refers to small-scale blending of various viscosity improvers. Ayhan [11] suggested that a 4% ethanol addition can reduce SVO viscosity by half and resolve the brake thermal efficiency reduction issues.

According to Ziejewski et al. [9], the performance issues as well as injector coking and other durability problems can be addressed with SVO thinners. More recently, Mikulski et al. [12] explored the possibility of using the light fraction of tire pyrolysis oil (TPO) as a viscosity improver for cold-pressed rapeseed oil. The fuel comprising of a 5% distilled TPO addition towards a 65/30 diesel - rapeseed oil mixture exhibited the quality close to the restrictive EN 590 standard for automotive diesel fuels. Moreover, the volatility characteristics of the DF/SVO mixture were improved while keeping the flash point limit of 55 °C. The blending study was supplemented by fuel performance and emission characterization conducted on an Euro VI, mid-duty common rail engine, reporting only slight reduction in efficiency and emissions with respect to the diesel baseline. At the same time, the TPO-doped DF/SVO mixture proved superior in terms of brake thermal efficiency and NO_X emissions over the benchmarked DF/FAME blend with a 20% share of renewable components.

The above-mentioned works by Ambrosewicz-Walacik et al. [8] and Mikulski et al. [12] are among the few that investigate the effects of SVO on reasonably modern CI engines with electronic fuel injection equipment. The remaining available literature pertains to studies investigating the SVO use case on very simple, legacy platforms that are characteristic of typical agricultural applications in less developed countries. Despite their contribution towards the understanding of individual effects related to SVO application, such results do not ultimately provide a proper benchmark with respect to the current emission standards. Furthermore, the scope of combustion/emission management enabled by the state of the art in CI engine controls opens up a new ground for SVO in relation to fuel-specific optimization of operation. Completing the list of knowledge gaps is the fact that only simple compounds have so far been tested as improvers for SVO. With the above opportunities and reinforced focus on the well-to-wheel greenhouse gases emission reduction, the problem of SVO fuel applications has attracted attention from researchers.

This work builds on the opportunities created by the above knowledge gaps and proceeds with state-of-the-art engine tests of a new SVO compound referred to as Plantanol™. The preliminary feasibility of the new fuel is tested on an Euro VIb light-duty CI engine. Single-cylinder engine tests are then focused on the optimization potential of injection parameters and external exhaust gas recirculation (EGR) to reach optimum performance-emissions trade-off on the new SVO compound. For brevity, the tested mixture is henceforth referred to as biofuel (BF).

Preliminary results and motivation

To verify the feasibility of the proposed BF for modern diesel engines, preliminary tests were carried out on a standard 4-cylinder, 2,000 cm^3 swept volume, light-duty automotive engine with Euro VIb parameterization. The investigations were performed at the Institute for Internal Combustion Engines and Powertrain Systems at the Technical University Darmstadt, Germany. The engine was operated with a stock engine control unit (ECU), and no adjustments were made to the control maps to accommodate for different characteristics of the tested fuels. Amongst a handful of stationary and transient test runs, the results of four representative steady-state operating points are shown in Fig. 1 to demonstrate the emission and performance footprint of the new fuel. It should be stressed that the brake values of mean effective pressure (BMEP) and thermal efficiency (BTE) are used to characterize the engine load and fuel economy.

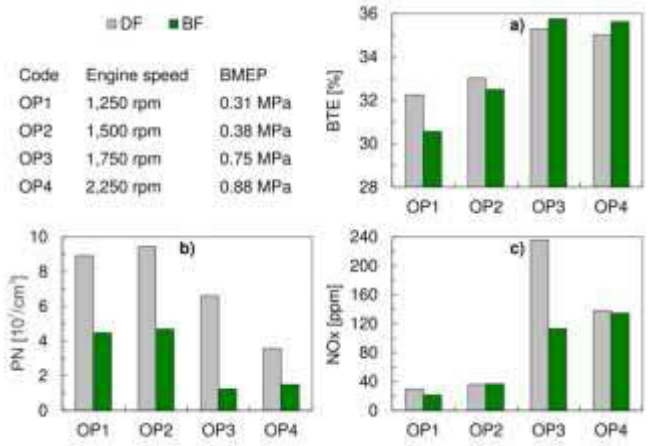

Figure 1. Preliminary results on a multi-cylinder engine at investigated operating points: brake thermal efficiency (a), particulate number (b) and concentration of NO_X (c).

As shown in Fig. 1a, the BF provides lower efficiency at low loads (OP1 and OP2) and higher efficiency at elevated loads (OP3 and OP4) when compared to the DF. Elevated viscosity of the BF (refer to Table 1) might cause efficiency losses due to increased parasitic losses in the fuel injection equipment or un-optimized combustion phasing [12]. While the latter effect is further investigated in the main part of this study, at this point it is important to notice the respective trends in NO_X (Fig. 1b) and particulates (Fig. 1c) emissions.

According to this preliminary benchmark conducted on the state-of-the-art automotive diesel engine, the commonly known particulates/NO_X trade-off can be relaxed with the proposed BF. The complex control actions of the multi-cylinder platform do not reveal the presence of mechanisms governing the potentially superior emission performance and differences in efficiency. Thus, detailed engine tests are performed on a dedicated single-cylinder engine platform with open ECU and with full thermal management of fuel and air-path. The details of the test platform and the experimental campaign are outlined in the next section. This is preceded by a detailed characterization of the tested fuels.

Materials and methods

Test fuels

Two test fuels are considered in this research: standard EN 590 mineral DF and BF composed of SVO and a viscosity improver (courtesy of Handelshaus Runkel). The SVO is a carefully selected blend of cold-pressed plant oils. The improver is also renewable-based, yet the details of the compound as well as respective compositions are company confidential. It should be noted that that the final BF sample contains 55 n/n% of triglycerides and the dominant concentrations of individual fatty acids in triglycerides are as follows: C18:1 – 64%, C18:2 – 17%, C18:3 – 7.3%, C16:0 – 4.2%. Finally, it should be stressed that neither DF nor BF contained any FAME. Table 1 gives the most relevant physicochemical parameters of both tested fuels.

The fuels considered in this study were characterized under laboratory conditions, according to the analytical procedures specified in the standards EN 590 and EN 14214 for mineral diesel and biofuels, respectively. For a more elaborate description of the employed laboratory methods, the reader is referred to the work by

Duda et al. [13]. Additionally, to highlight the effect of the improver, the tested BF was compared with the typical properties of a neat SVO taken from the literature [12].

Table 1. Properties of tested fuels.

Parameter	Unit	DF	BF	SVO**
Density @ 15 °C	g/ml	0.837	0.867	0.920
Viscosity @ 40 °C	mm^2/s	2.94	11.2	39
LHV	MJ/kg	42.8	38.2	36.1
Stoichiometric AFR	kg/kg	14.73	13.27	12.47
Flash point	°C	70.5	41	>200
Oxidative stability	h	> 22	> 6	6.47
CFPP*	°C	-22	-9	n.d.
Acid value	mg KOH/g	0.07	0.21	2
Sulfur content	mg/kg	6.1	9.04	7.1

* Cold filter plugging point.

** Reference value for cold-pressed rapeseed oil from the literature [12].

From Table 1, it can be seen that the physicochemical properties of both tested fuels differ to a great extent. The density of BF is slightly higher than that of diesel yet its mass-based LHV is roughly 11% lower, which translates directly to higher specific fuel consumption. However, the lower LHV of BF is caused by higher oxygen content, which in turn reduces stoichiometric air-fuel ratio (AFR). Therefore, the differences between the heating values of stoichiometric mixtures are diminished, namely 2.72 MJ/kg for DF and 2.68 MJ/kg for BF. It must be highlighted that the density of BF was improved to match the requirements of EN 14214. The viscosity of BF is still far from that of DF, but an over 70% reduction is obtained with respect to the SVO baseline, allowing combustion in the CI engine without fuel pre-heating. Owing to major differences in viscosity, an effect on ignition delay and atomization should be expected, with further impact on efficiency and emissions. The effect of the viscosity improver is also evident in the heavily lowered flashpoint. The trade-off is evident here, and the viscosity improvement gives rise to fuel safety handling issues – which is a well-known problem [12].

Summing up, the BF under study does not meet the requirements of EN 590, yet most of the quantifiers are compliant with the EN 14214 standard specifying the quality requirements for biodiesels. This is with the exception of viscosity which is still over 100% higher than that of the referenced standard.

Single-cylinder engine setup and procedures

Single-cylinder engine tests were performed at the Lublin University of Technology, Poland. An AVL four-stroke, light-duty single-cylinder CI engine type 5402 CRDI was used as the research object. The test engine specifications are given in Table 1. The engine had a toroidal, in-piston combustion chamber with swirl. The cylinder head had a four-valve design with a swirl port (AVL-LEADER concept).

The engine was coupled with an asynchronous motor dynamometer with speed control. The test stand was also equipped with coolant- and lubricant-conditioning systems to ensure constant temperature conditions, independent of the operating point. The test stand automation system was based on a programmable logic controller and in-house software.

The experiments were performed at mid-load regime, with the engine operated as naturally aspirated. Exhaust gas was recirculated via a butterfly valve and a cooler providing a constant EGR temperature at the entrance to the intake manifold. An exhaust backpressure valve was installed downstream of the exhaust plenum to enable high EGR rates.

Table 2. Single-cylinder engine data.

Type	AVL 5402
Configuration	single-cylinder, 4-stroke
Bore	85 mm
Stroke	90 mm
Displacement	510 cm^3
Compression ratio	17:1
Number of valves	4
Injector	Seven-hole
Max. fuel pressure	180 MPa
Injection system	Common Rail Bosch CP4.1
Engine management	AVL, ETK7-Bosch
Inlet valve opening	712 °CA
Inlet valve closing	226 °CA
Exhaust valve opening	488 °CA
Exhaust valve closing	18 °CA

The fuel delivery system consisted of the AVL 733S dynamic fuel meter and 753C fuel temperature conditioner. Additionally, an intake air thermal mass flow meter and low-frequency pressure and temperature transducers were installed in the intake runner, exhaust manifold, EGR path, cooling and lubrication systems. Concentrations of gaseous components in the exhaust gas were measured using the AVL Fourier transform infrared (FTIR) multi-compound analytical system. PM concentrations were measured with the Maha MPM-4 analyzer. The excess air ratio (λ) was measured with the LSU 4.2 Bosch lambda probe and the ETAS LA4 lambda meter. Intake gas was sampled from an intake plenum chamber and analyzed using the Hermann-Pierburg HGA 400 gas analyzer. The EGR rate was estimated using an intake/exhaust CO_2 ratio.

The combustion analysis was based on in-cylinder pressure measurements. For this purpose, the AVL GU22C pressure transducer was installed directly in the engine head and connected via a charge amplifier to the test bench acquisition system. The high-speed pressure recording was triggered via an optical encoder, with a constant resolution of 0.1 ° crank angle (CA). The acquisition system for the test bench was PC-based with dedicated in-house software. In-cylinder pressure at each measurement point was acquired for 100 consecutive cycles and then averaged. The first law thermodynamic analysis was performed to compute the heat release rate (HRR). The Hohenberg correlation was used to evaluate the heat transfer coefficient.

Mechanical losses of the engine were not considered in the study, so fuel consumption was provided as indicated-specific. Directly measured molar concentrations of exhaust gas components were converted to indicated specific emissions, taking into account the specific fuel consumption and the exhaust gas chemical composition. PM emissions were recorded as mass per volume units with a

measuring device, so that exhaust density and fuel consumption could be considered to calculate emission factors.

Experimental matrix

The experiments focused on exploring a single, mid-load operating point. The rotational speed of the engine was maintained constant at 2000 rpm and the net IMEP was around 0.45 MPa. The engine was run as naturally aspirated, with ambient intake pressure. Note that at each operating point the injector's pulse durations were corrected to maintain desired IMEP. Therefore excess air ratio (λ) was not explicitly controlled. Temperatures of the engine coolant and the lube oil were set at 85 °C. The EGR temperature was maintained constant at 85 °C. The fuel rail pressure was 80 MPa and the fuel temperature was 30 °C in all experiments.

The experimental matrix consisted of various split fuel injection strategies explored at different EGR rates. The start of pilot injection (SOIp) was shifted 5°CA left and right from its respective baseline position at 335 °CA. This was applied as an effective measure to influence the combustion phasing, as verified in previous work by Hunicz et al. [14]. The main fuel start of injection (SOIm) was set constant to 352 °CA. Note that all timings are given after the top dead center (TDC) in the valve overlap period. At these three SOI timing configurations, the fuel ratio between the pilot and the main injection was swept in order to adjust the NO_X and soot trade-off for different fuels. The whole procedure was repeated for non-EGR conditions and the external EGR rate set to approximately 25%. Additionally, a full EGR sweep in the baseline injection conditions was performed to illustrate the engine response to EGR.

The next section discusses the effects of the above-described injection and EGR measures (the order is preserved) on the engine performance and emissions characteristics when operating on BF. Results obtained for DF are provided as a reference. It is worth noting that the above-mentioned baseline injection parameters: SOIp = 335 °CA, SOIm = 352 °CA and the fuel split ratio of 15% (pilot fuel mass vs total fuel value), were inspired by the factory ECU settings of the investigated multi-cylinder engine at the respective load/speed operating point.

Results and discussion

Pilot fuel SOI sweep

Figure 2 shows the measured in-cylinder pressure and calculated HRR traces for both fuels at different SOIp values and under non-EGR conditions. The results obtained for BF are indicated in green, while the respective DF baseline is marked with black lines.

One can observe that BF generally ignites earlier considering low-temperature reactions associated with the early pilot. The lower cumulative heat release in this stage causes that this advance is lost in favor of DF during the main combustion event. For BF this phase starts later and is characterized by a substantially longer duration. This can clearly be seen in Fig. 1b and is manifested in Fig. 1a as reduced peak pressure values for BF. It should be noted that regardless of the fuel used, the later the SOIp occurs, the more heat is released from the pilot fuel, which consequently advances the combustion of the main fuel.

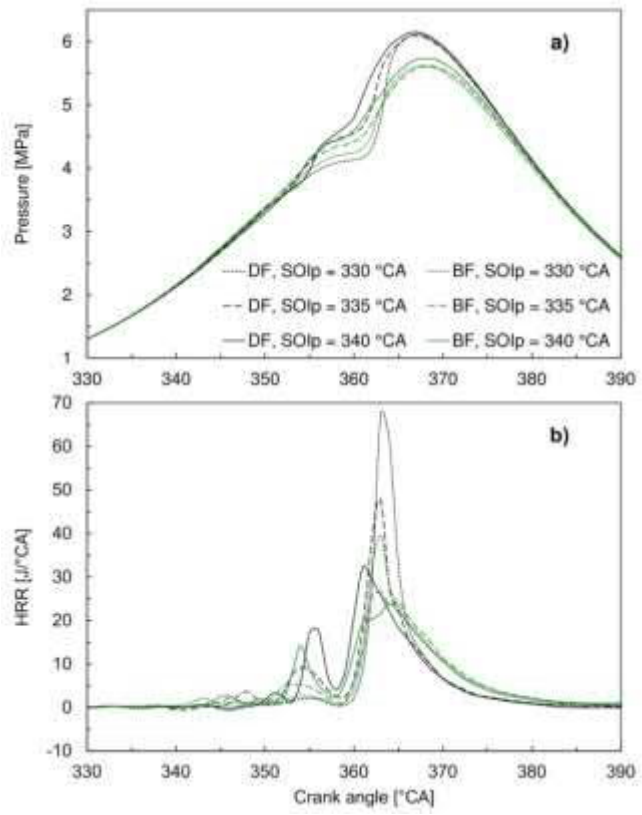

Figure 2. In-cylinder pressure (a) and HRR (b) for different SOIp timings; 15% pilot fuel injection, non-EGR conditions.

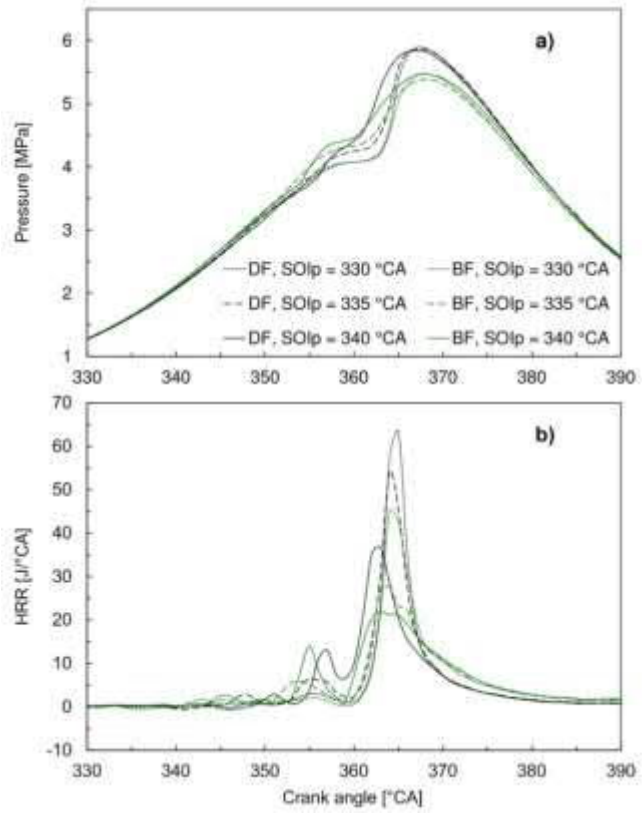

Figure 3. In-cylinder pressure (a) and HRR (b) for different SOIp timings; 15% pilot fuel injection, 25% EGR conditions.

The main trends in combustion are replicated for the 25% EGR case, as outlined in Fig. 3. There are, however, some important quantitative differences. For instance, for BF the combustion is less complete as it still progresses late at CA ≈ 390 °CA (positive HRR in Fig. 2b). Furthermore, an interesting trend is observed for the EGR case, namely –the pilot fuel provides roughly the same early-stage cumulative heat release for both fuels. The accelerated main combustion ignition for DF evident in Fig. 3b results from the fact that the SOIm spray develops into progressing combustion of the pilot fuel.

The above brief discussion on combustion characteristics of both fuels can be wrapped up with some considerations on the efficiency and emissions plotted in Fig. 4. Comparing fuel-to-fuel in the non-EGR scenario, the differences in indicated thermal efficiency (ITE) are just above the level of significance for the advanced and retarded pilot injection scenario (0.4 percentage points in favor of DF). For the nominal case (SOIp at 335 °CA) the difference diminishes and is within the maximum error of ITE determination of 0.2 pp. At this point, it is necessary to mention that the error was calculated from the maximum uncertainties of directly measured quantities comprising ITE, using the exact differential method. For details on the method, the reader is referred to Mikulski et al. [12]. The slight deterioration of ITE while switching to BF can be attributed to elongated and incomplete combustion. Compare the CA50 values of the non-EGR cases for the 15% split ratio in Fig. 5, and the THC/CO emission results in Fig. 9 for reference.

With regard to emissions, the EGR cuts down the NO_X by roughly 60-70% for both fuels, which is attributed to reduced excess air (lower oxygen content) and reduced combustion temperature. For instance, for the SOIp at 335 °CA and non-EGR conditions λ was 2.61 for DF and 2.53 for BF. For the 25% EGR the λ values were 1.83 and 1.79 respectively. Note that for BF λ is slightly lower compared to DF due to SVO-bounded oxygen – the effect of adopted fueling strategy (constant IMEP).

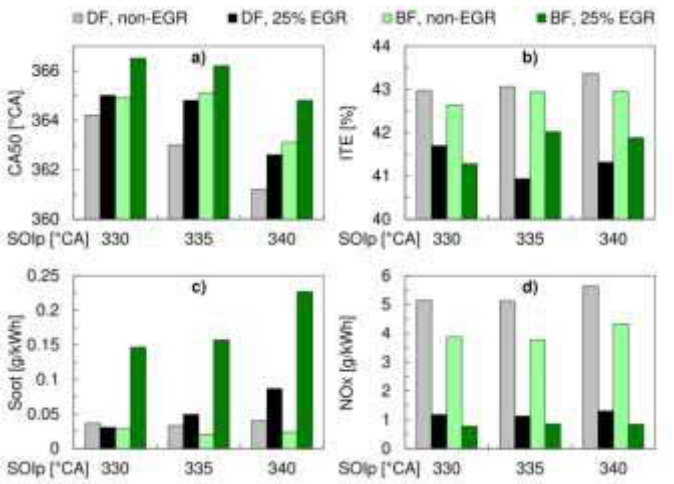

Figure 4. Location of 50% MFB (a), indicated specific fuel consumption (b), soot emissions (c) and NO_X emissions (d) for different SOIp timings; 15% pilot fuel injection.

The combustion of BF results in considerably lower engine-out NO_X compared to DF. Considering the above remarks on λ, the effect is thermal-related. Reduced peak pressures (see Fig. 2 and Fig. 3 for reference) for BF result in lower bulk cylinder temperatures suppressing the thermal NO creation. The soot emission is also slightly reduced for BF, compared to that obtained for DF, however it is observed solely for the non-EGR case. The EGR operation on BF results in excessive PM emissions with their values ranging from 0.15 to 0.22 g/kWh depending on the SOIp. To give an example, the DF baseline produced the engine-out PM below 0.03 g/kWh, while the Euro VI limit is an order of magnitude lower (0.005 g/kWh).

In all cases an increase in EGR also causes deterioration of ITE due to retarded combustion. According to the same mechanism, ITE generally decreases while moving towards early SOIp. For DF, at late SOIp angles, a better performance means some trade-off in terms of both soot and NO_X. BF generally reacts in a similar manner, but there occurs some non-monotonic behavior at SOIp = 335 °CA. This is manifesting particularly for the EGR case, where the ITE is almost 1 pp higher for BF compared to DF baseline. For BF the SOIp at 335 °CA resulted in the best performance/emission tradeoff. Consequently, the behavior pattern observed at this injection strategy is thoroughly discussed in the next subsection in order to address other combustion optimization measures.

Fuel split ratio sweep

In the previous section, Fig. 2 and Fig. 3 provided insight into the combustion characteristics of both tested fuels and explained how the split injection affected the combustion phasing. For brevity, this is further synthesized into a CA50 plot. For the fuel split ratio sweep, this is presented in Fig. 5.

Coupling the observations based on heat release analysis with the results in Fig. 5 explains the superior ITE for the BF under EGR. At such conditions the CA50 is retarded only slightly with respect to DF (Fig. 5, EGR case, pilot fraction 15%), yet the BFs early HRR is considerably reduced (Fig. 3b) causing less negative work on the piston before TDC. Result is roughly 1 pp higher ITE for the BF at SOIp = 335 °CA.

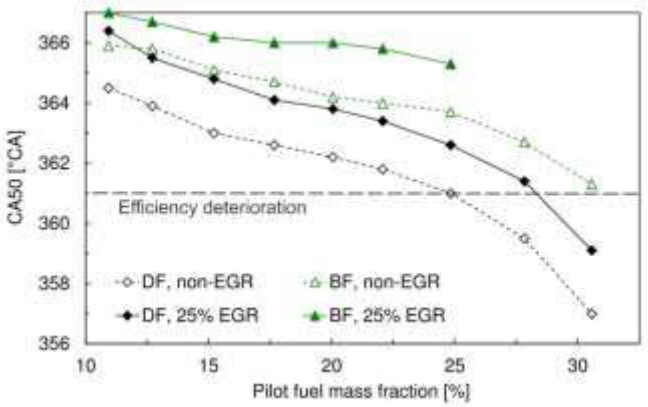

Figure 5. Location of 50% MFB for variable pilot fuel mass fraction; SOIp = 335 °CA.

As far as observed trends are concerned, changing the pilot fuel quantity produces a similar effect, regardless of the SOIp angles, EGR conditions or fuel type. Increasing the pilot fraction has two main effects. First of all, it accelerates the main combustion event because the SOIm develops into a hotter burned zone of the pilot. The accelerated main combustion improves efficiency. Secondly, the higher share of the cumulative heat release associated with the pilot occurs early in the compression phase, which results in reduced efficiency. Due to these contracting effects, the ITE remains highly insensitive to the changes in combustion phasing in spite of the fact

that the overall CA50 improves with increasing the pilot, as shown in Fig. 5. This trend is sustained until CA50 drops below around 361 °CA, where a rapid decrease of the ITE was observed due to high fuel fraction burnt before TDC. For instance, for the non-EGR DF case, the ITE dropped from 40.8% at 25% split ratio, consistently around 0.3 pp per 5 pp increase in the pilot fuel fraction.

The above discussion allows to decouple the BF optimization problem and, as long as the efficiency deterioration boundary (marked in Fig. 5) is not exceeded, narrow it down to the emission problem solely. To this end, Fig 6. shows the trends in soot and NO_X emissions under non-EGR conditions and selected SOIp of 335 °CA. Figure 7 shows the corresponding trends for the 25% EGR case.

Figure 6 shows that in the case of DF, the split ratio does not enable virtually any further optimization potential. The results obtained for BF show that the soot emissions are sensitive to the change in the pilot fraction; however, the minimum value is still achieved for the baseline split ratio point set at 15%. At this point, the BF scores roughly 28% and 41% lower NO_X and Soot emissions, respectively, when compared to the diesel reference.

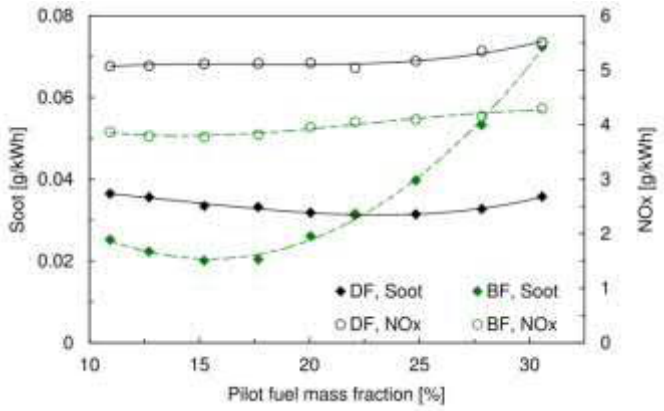

Figure 6. Emissions of soot and NO_X for variable pilot fuel mass fraction; SOIp = 335 °CA, non-EGR conditions.

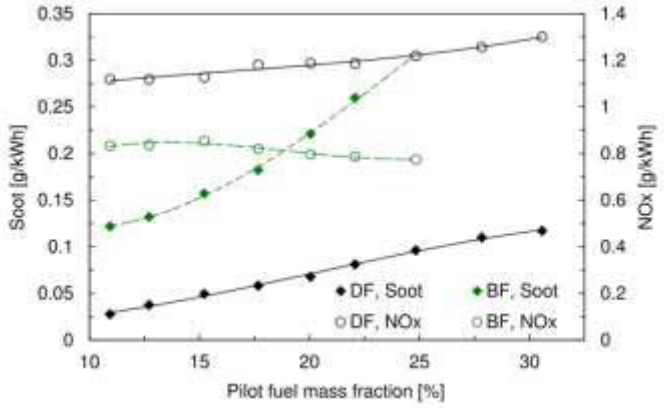

Figure 7. Emissions of soot and NO_X for variable pilot fuel mass fraction; SOIp = 335 °CA, 25% EGR conditions.

Figure 7 shows that the addition of 25% EGR makes it possible to reduce the soot emissions for BF while moving from the diesel baseline split ratio towards short pilot injections. This change of the injection strategy does not affect the NO_X emission, as it remains far below the 1.2 g/kWh level set for the DF stock optimization. However, for BF the optimized soot emission is still over 150% higher than that of the diesel EGR baseline. It should be noted that according to Fig. 7, the DF/EGR operation could be further optimized in terms of soot emissions while progressing toward smaller split ratios. However, in this case, reducing the pilot fuel fraction below 11% results in a rapid increase in the cycle-to-cycle variations because the injector is operated close to the ballistic region. With the mass-based LHV being roughly 11% lower for BF, at the same split ratio a longer pilot injection is realized and thus stable operation is sustained for BF toward small pilot injections.

EGR ratio sweep

The discussion in the preceding sections suggests a high sensitivity of BF emissions to EGR. The observations made so far can be summarized with a statement that BF performs satisfactorily in the non-EGR conditions yet responds with high soot emissions at elevated EGR rates. Fig. 8 provides more insight into this problem.

If low NO_X calibration is required, EGR is applied. The application of EGR reduces the compression temperature (lower ratio of specific heats) and reduces excess air, which drastically cuts down on NO_X yet causes extended ignition delay and retarded combustion, which leads to lower efficiency as well as reduced THC and CO emissions. In CI engines, the EGR limit is usually set to keep smokeless operation (related to soot emissions). From Fig. 8 it can be seen that for the mid-load operating point in DF operation, the low soot limit can be maintained up to around 25% EGR. On the other hand, BF reaches this limit at around 20% EGR, followed by a further decrease in the air-fuel ratio, which causes a rapid increase in soot production. It should, however, be noted that at this setting BF has roughly the same NO_X output as diesel at 25% EGR.

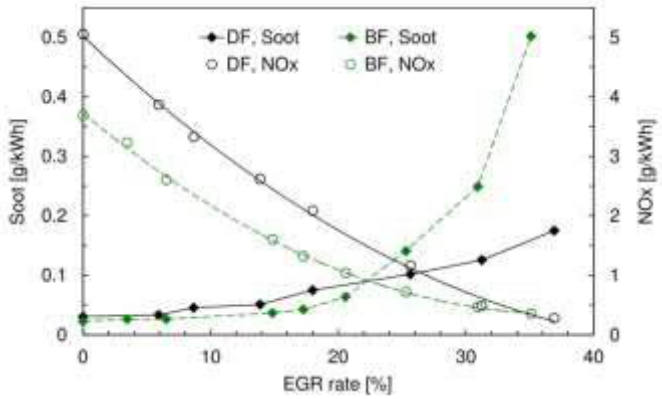

Figure 8. Emissions of soot and NO_X for variable EGR rates; 15% pilot fuel injection, SOIp = 335 °CA.

Detailed exhaust speciation

The discussion above was focused on the efficiency/NO_X/PM dilemma as a major issue regarding the applications of alternative fuels in CI engine. For a complete picture, it is however important to quantify the performance of the examined BF with respect to other emission factors. Fig. 9 presents the emission results for CO and THC, together with a detailed analysis of specific hydrocarbons and other compounds detected by the FTIR analyzer. For brevity, the benchmark of BF against DF is limited to the baseline operating point.

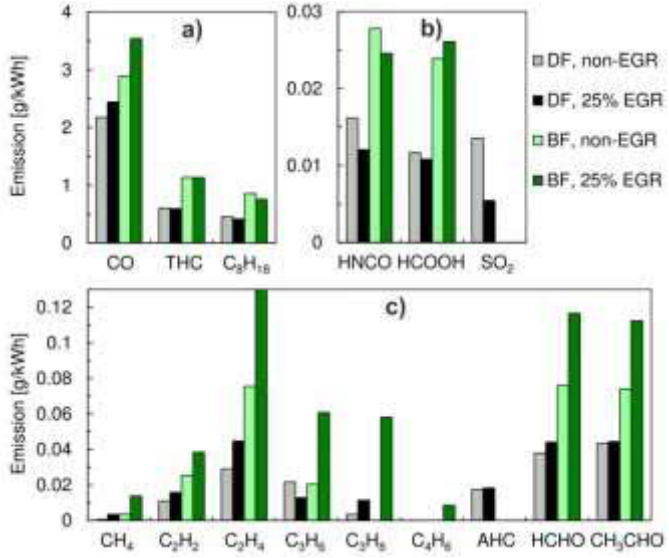

Figure 9. Emissions of selected regulated and non-regulated compounds; 15% pilot fuel injection, SOIp = 335 °CA.

According to Fig. 9, both the CO and THC emissions are significantly higher for BF than for DF. This can be attributed to higher viscosity resulting in worse fuel atomization and reduced oxygen entrainment into the developing spray. The observation is consistent with the majority of reports concerning SVO utilization [7]. To extend on this knowledge, the present study reveals how the elevated THC is distributed between particular hydrocarbons.

Fig. 9 suggests that THC primarily consists of C-8 chains. Under EGR conditions the C_8H_{18} emission is slightly reduced in favor of lighter hydrocarbons. The same trend is observed for both examined fuels, but the quantitative effect is multiplied for BF. Among light hydrocarbons, acetylene (C_2H_2) is a challenge, because it inhibits oxidation of other hydrocarbons in a catalytic converter, especially at low temperatures, at the light-off threshold [15]. Acetylene emission was doubled for BF. The biofuel ultimately produces 100%-150% more aldehydes. These unlegislated species pose a growing concern for heavy duty diesel engines [16] and should be considered when assessing fuel feasibility. It should be noted that formaldehyde (HCHO) and acetaldehyde CH_3CHO) are at the same level, yet BF is more sensitive to EGR in terms of cumulative aldehyde emissions. Also, formic acid (HCOOH) is increasingly present in the BF combustion products. This is due to the carboxylic acids content in the fuel itself. Besides its propensity to create teratogenic methanamide, formic acid – when entered into a reaction with other combustion products – is extremely corrosive, which may pose maintenance problems and produce a poisoning effect in catalytic converters [17].

On the pros side, BF does not produce any aromatics or SO_2. Since BF does not contain aromatics, they are not present in the exhaust. However, the emission of SO_2 is different for both fuels. While the reduction in the SO_2 emissions for DF when EGR is applied can be explained by the bounding of some fuel sulfur in particulates, BF does not produce any sulfur, not even under non-EGR conditions, although it is present in the fuel.

Conclusions

This work investigated the feasibility of using viscosity-improved straight vegetable oil (Plantanol™) as an inexpensive and CO_2-advantagous alternative to refined biofuels. The test campaign on a contemporary Euro VIb engine with standard control maps has confirmed that it is feasible, revealing that the fuel has a lower propensity to produce soot while the NO_X emission is on a similar level to that of the diesel baseline. Dedicated single cylinder tests provided further insight into the phenomena, leading to the following conclusions:

1. In the divided injection strategy, the tested biofuel exhibits faster early stage combustion due to a higher Cetane Number. The main diffusion-controlled combustion phase is heavily prolonged due to high viscosity of the fuel.
2. The changes in the course of combustion are the main reason for the observed reduction in soot-NOx emissions under non-EGR conditions. The tested fuel exhibits roughly 28% and 41% lower NO_X and Soot emissions, respectively, when compared to the diesel reference.
3. The fuel reacts more rapidly to EGR, and low NO_X calibration is achieved at lower EGR rates, providing efficiencies 1 percentage point higher than DF. At the EGR rate above 25%, which is a standard low-NO_X setting for diesel, the engine operates at a visible smoke limit with excessive soot emission.
4. For optimum emissions, the EGR rate should be reduced to 20% while operating on the tested biofuel solution. The benefits of a wider injection optimization window can be incorporated here, since the ballistic injector operation is achieved at lower split ratios than is the case with diesel.
5. On the cons side, the elevated CO and THC emissions are potential short-stoppers for the Plantanol fuel roadmap. Although they can be relatively easily oxidized in the DOC (diesel oxidation catalyst), the high aldehyde and formic acid content in the exhaust gases might negatively influence the catalyst performance over lifetime.

References

1. Energy demand: Three drivers. ExxonMobil 2019. https://corporate.exxonmobil.com/Energy-and-environment/Looking-forward/Outlook-for-Energy/Energy-demand#transportation . Access 10 Oct. 2019.
2. Gebremariam, S.N. and Marchetti, J.M., "Economics of Biodiesel Production: Review," *Energy Conversion and Management*. 168:74-84, 2018, doi:10.1016/j.enconman.2018.05.002.
3. Hossain, A.K. and Davies, P.A., "Plants Oils as a Fuels for Compression Ignition Engines: a Technical Review and Life Cycle Analysis," *Renewable Energy*. 35(1):1-13, 2010, doi:10.1016/j.renene.2009.05.009.
4. Agarwal, D., Kumar, L. and Agarwal, A.K., "Performance Evaluation of a Vegetable Oil Fuelled Compression Ignition Engine," *Renewable Energy*. 33:1147-1156, 2008, doi:10.1016/j.renene.2007.06.017.
5. Ortner, M.E., Müller, W., Schneider, I. and Bockreis, A., "Environmental Assessment of Three Different Utilization Paths of Waste Cooking Oil From Households," *Resources. Conservation and Recycling*. 106:59-67, 2016, doi:10.1016/i.resconrec2015.11.007.
6. Esteban, B., Baquero, G., Puig, R., Riba, J.R. and Rius, A., "Is it Environmentally Advantageous to Use Vegetable Oil Directly as Biofuel Instead of Converting it to Biodiesel?" *Biomass Bioenergy*. 35(3):1317-1328, 2011, doi:10.1016/j.biombioe.2010.12.025.
7. Misra, R.D. and Murthy, M.S., "Straight Vegetable Oils Usage in a Compression Ignition Engine – Review," *Renewable and*

Sustainable Energy Reviews. 14(9):3005-3013, 2010, doi:10.1016/j.rser.2010.06.010.
8. Ambrosewicz-Walacik, M., Wierzbicki, S., Mikulski, M., and Podciborski, T., "Ternary Fuel Mixture of Diesel, Rapeseed Oil and Tire Pyrolytic Oil Suitable for Modern CRDI Engines," *Transport*. 33(3):727-740, 2018, doi:10.3846/transport.20185163.
9. Ziejewski, M., Goettler, H. and Pratt, G., "Comparative Analysis of the Long-Term Performance of a Diesel Engine on Vegetable Oil Based Alternate Fuels," SAE Technical Paper 860301, 1986, doi:10.4271/860301.
10. Devan, P.K. and Mahalakshmi, N.V., "Performance, Emission and Combustion Characteristics of Poon Oil and its Diesel Blends in a DI Diesel Engine," *Fuel*. 88:861-867, 2009, doi:10.1016/j.fuel.2008.11.005.
11. Ayhan, D., "Progress and Recent Trends in Biodiesel Fuels," *Energy Conversion and Management*. 50:14-34, 2009, doi:10.1016/j.enconman.2008.09.001.
12. Mikulski, M., Ambrosewicz-Walacik, M., Duda, K. and Hunicz, J., "Performance and Emission Characterization of a Common-Rail Compression-Ignition Engine Fuelled with Ternary Mixtures of Rapeseed Oil, Pyrolytic Oil and Diesel," *Renewable Energy*. 148:739-755, 2020, doi:10.1016/j.renene.2019.10.161.
13. Duda, K., Wierzbicki, S., Śmieja, M. and Mikulski, M., "Comparison of Performance and Emissions of a CRDI Diesel Engine Fuelled with Biodiesel of Different Origin," *Fuel.* 212:202-222, 2018, doi: 10.1016/j.fuel.2017.09.112.
14. Hunicz, J., Matijošius, J., Rimkus, A., Kilikevičius, A. et al. "Efficient Hydrotreated Vegetable Oil Combustion Under Partially Premixed Conditions with Heavy Exhaust Gas Recirculation," *Fuel.* 268:117350, 2020, doi:10.1016/j.fuel.2020.117350.
15. Hunicz, J. and Medina, A., "Experimental Study on Detailed Emissions Speciation of an HCCI Engine Equipped with a Three-way Catalytic Converter," *Energy* 117:388-397, 2016, doi:10.1016/j.energy.2016.06.049.
16. Rodrigues, M.C., Guarieiro L.L.N., Cardoso, M.P., Carvalho, L.S. et al., "Acetaldehyde and Formaldehyde Concentrations from Sites Impacted by Heavy-Duty Diesel Vehicles and Their Correlation with the Fuel Composition: Diesel and Diesel/Biodiesel Blends," *Fuel* 92(1):258-263, 2012, doi:10.1016/j.fuel.2011.07.023.
17. Nova, I. and Tronconi, E., "Urea-SCR Technology for deNOx After Treatment of Diesel Exhausts," Springer Science & Business Media, 2014, ISBN:1489980717.

Contact Information

Jacek Hunicz
Lublin University of Technology, Nadbystrzycka 36, 20-618 Lublin, Poland
e-mail: j.hunicz@pollub.pl

Acknowledgments

The part of the research conducted at the Lublin University of Technology was financed in the framework of the project Lublin University of Technology Regional Excellence Initiative, funded by the Polish Ministry of Science and Higher Education (contract No. 030/RID/2018/19).

Definitions/Abbreviations

AFR	Air-fuel ratio
BF	Biofuel
BMEP	Brake mean effective pressure
BTE	Brake thermal efficiency
CA	Crank angle
CA50	Crank angle of 50% MFB
CI	Compression ignition
DF	Diesel fuel
EGR	Exhaust gas recirculation
FAME	Fatty acid methyl ester
HRR	Heat release rate
HVO	Hydrotreated vegetable oil
IMEP	Indicated mean effective pressure
ITE	Indicated thermal efficiency
LHV	Lower heating value
MFB	Mass fraction burned
SOIm	Main fuel start of injection
SOIp	Pilot fuel start of injection
SVO	Straight vegetable oil
TDC	Top dead center
THC	Total hydrocarbons